Optical Coherence Tomography Imaging of Cardiac Trabeculae

Ming L. Cheuk, *Student Member, IEEE*, Norman Lippok, Alexander W. Dixon, Bryan P. Ruddy, *Member, IEEE,* Frédérique Vanholsbeeck, Poul M.F. Nielsen, *Member, IEEE,* and Andrew J. Taberner, *Member, IEEE*

***Abstract*— An integrated instrument is being developed to study live cardiac trabeculae, which is capable of stimulating the muscle under controlled conditions while measuring the heat production, force, and sarcomere length distribution. To improve the accuracy of estimation of stress, strain, and volumetric heat production, the geometry of the muscle must be known. A spectral domain optical coherence tomography system (SD-OCT) has been constructed and calibrated to image the trabecula mounted inside the instrument. This system was mounted above the muscle chamber and a series of equally-spaced cross-sectional images were obtained. These were processed using a workflow developed to extract cross-sectional area and volume. The initial results have demonstrated the feasibility of using OCT to capture the overall geometry of cardiac trabecula mounted in the instrument. Further work will be directed to improve the image quality for larger samples and apply meshing algorithms to the acquired data.**

I. Introduction

Factors such as disease and drugs can cause changes in the intracellular mechanisms contributing to heart contraction. To study these changes, we are building an integrated testing device capable of performing mechanical, calorimetric, and intracellular calcium measurements on bundles of cardiac myocytes. The instrument is designed to be used with cardiac trabeculae – rod shaped muscle tissue found in the ventricles of the heart. Their shape and composition make them ideal choices for studying cardiac muscle in vitro [1,2].

Each dissected specimen has a unique shape that has to be characterized for accurate calculation of stresses and strains developed within the tissue [3]. Studying 2D geometry of the trabecula's silhouette is currently possible with a light microscope, but until now no accurate measurement of 3D shape and deformation was possible. This paper investigates the use of OCT to measure 3D geometry of trabecula mounted in the instrument, and presents preliminary results from a processing algorithm developed to extract area and volume from the OCT images.

*Research supported by the Marsden Fund Council from Government funding, administered by the Royal Society of New Zealand (#UOA1108)

M. L. Cheuk (Tel: +64220314159 Email: ming.cheuk@auckland.ac.nz) and A. W. Dixon are with the Auckland Bioengineering Institute, New Zealand.

N. Lippok is with the Auckland Bioengineering Institute and The Department of Physics, University of Auckland, New Zealand.

F. Vanholsbeeck is with The Department of Physics, University of Auckland, New Zealand.

B. P. Ruddy, P. M. F. Nielsen, and A. J. Taberner are with the Auckland Bioengineering Institute and The Department of Engineering Science, University of Auckland, New Zealand.

II. Optical Coherence Tomography

OCT is an interferometric technique that provides depth-resolved, cross-sectional images of tissue reflectance. In OCT, a beam of light with a short coherence length illuminates the sample and reflections from within the sample are recorded. Using the interferometric signal, the reflected signals can be separated, based on the path difference with the refenece arm, to build a depthwise intensity profile of scattering particles. The beam may be steered laterally and longitudinally about the sample to build a full 3D intensity profile.

The translucency and scattering properties of most biological tissues make them ideal candidates for OCT imaging. OCT has found its way into many biomedical research and clinical applications, including retinal, intravascular, and gastrointestinal imaging for diagnosis or study of various pathologies [4]. A major advantage of OCT is that no special preparation of the sample is required. Most OCT systems can image to a tissue depth of at least 1 mm [5,6], enabling us to resolve the entire trabecula in one scan without adjusting the position of the sample.

III. Methods

A. Construction

A spectral domain OCT (SD-OCT) was assembled for imaging trabeculae. Figure 1 depicts the system. A superluminescent diode with a center wavelength of 840 nm and a spectral width of 90 nm (Broadlighter D-840, Superlum) is used as the source. A 2D galvanometer steers the laser through the specimen (GVSM002/M, Thorlabs). The reflected light is collected and combined with a

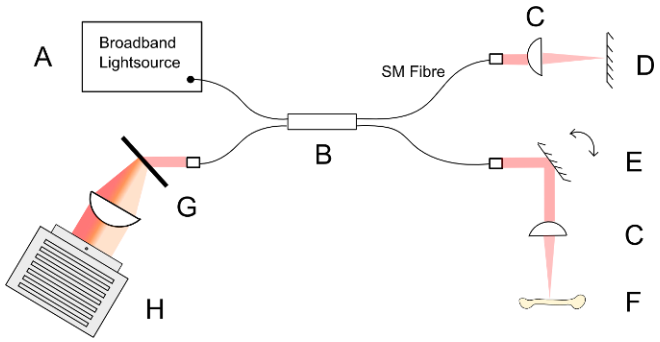

Figure 1. Schematic of constructed OCT system. (A) Broadband light source. (B) 2 x 2 Fibre coupler. (C) Converging lens. (D) Reference mirror. (E) Scanning mirror galvanometer. (F) Specimen. (G) Holographic grating. (H) Line scan camera.

978-1-4244-7929-0/14/$26.00 ©2014 IEEE

reference beam using a 2 x 2 fibre coupler (FC850-40-50-APC, Thorlabs). The interfered signal is diffracted through a transmission volume phase holographic grating and the spectrum is captured on a 2048 pixel line scan camera (spL2048-70km, Basler).

The coherence length of the source gives an axial resolution of 3.6 µm in air [7]. The lateral resolution is limited by the beam waist, which depends on the illumination wavelength, the diameter of the collimated beam, and the focal length of the objective lens. The system uses an achromatic doublet lens with a focal length of 50 mm, giving a lateral resolution of 23 µm [8].

A new muscle bath was constructed to simulate mounting conditions in the device. The bath uses a very similar design to that of our previous calorimeters [1,8] and was fabricated by 3D printing in ABS plastic. The sample chamber was constructed from a square glass capillary with an inner width of 1 mm and wall thickness of 0.2 mm. Platinum hooks fabricated using wire electrical discharge machining were used to mount the muscle. These hooks were attached to micromanipulators, allowing position adjustments in three orthogonal axes.

The sample arm of the OCT was mounted at 10° to the surface of the muscle bath to reduce the intensity of light reflecting off the surface of the glass capillary, which otherwise can cause signal saturation and autocorrelation artifacts to appear in the image. The sample arm was attached to a linear stage that allows for adjustment of the axial distance.

B. *Software*

LabVIEW was used to acquire signals and control the galvanometer. In the acquisition routine, the spectrum is acquired, linearized and the Fast Fourier Transform (FFT) is taken to produce a single depth-wise intensity profile (A-scan). This is repeated at every increment of the galvanometer and the images are saved to the hard disk. The software can acquire and process A-scans at up to 15 kHz.

C. *Calibration*

The depth scan was calibrated using a reference glass slide. The two surfaces of the slide were imaged and the calibration factor was found to be 1 pixel per 3.17 µm length equivalent in air. Different refractive indices will change the path length of the beam. This effect can be accounted for if the refractive index of the sample is known. The refractive index for muscle tissue is estimated to be about 1.37 [10].

The lateral spacing between individual A-scans was found using a negative 1951 USAF resolution test target. 4 mV increments in voltage were applied to the galvanometer to steer the beam across the target. The displacement at each increment was found to be 6.73 µm.

D. *Experimental Procedure*

Unbranched trabeculae were micro-dissected from the right ventricle of adult Wistar rats with small blocks of ventricular wall at each end [11]. Trabeculae were then transferred to a chamber, pinned at stretched length, and fixed for 10 minutes in 2 % paraformaldehyde (PFA) diluted with phosphate buffered saline (PBS) at room temperature. Fixed trabeculae were then stored in PBS at 4 °C until imaged. The bulk tissue at the ends was trimmed before imaging to allow the sample to be mounted between the platinum hooks. The sample was mounted in the capillary filled with Tyrode's solution (Figure 3). The OCT beam was steered through the specimen and a total volume of 3 mm × 1.5 mm × 1.5 mm was imaged (x × y × z).

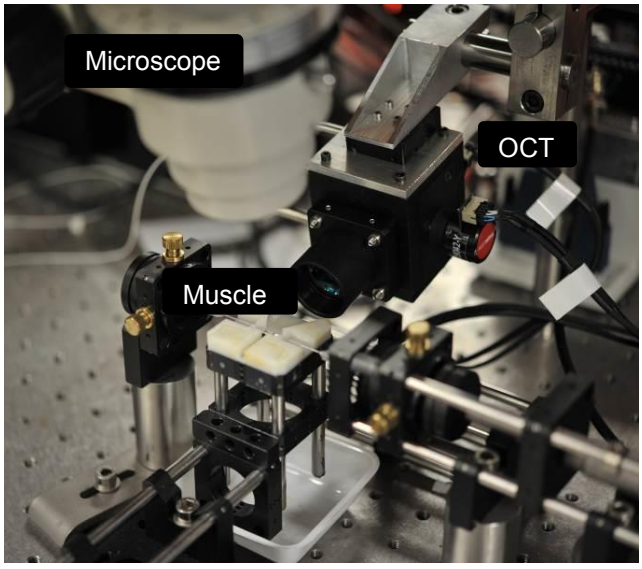

Figure 2. The setup used in this experiment. The trabecula is mounted on platinum hooks inside the glass capillary at the center of the muscle bath. The OCT is imaged 10 ° from the horizontal plane. The microscope above the bath is used to assist for mounting the muscle.

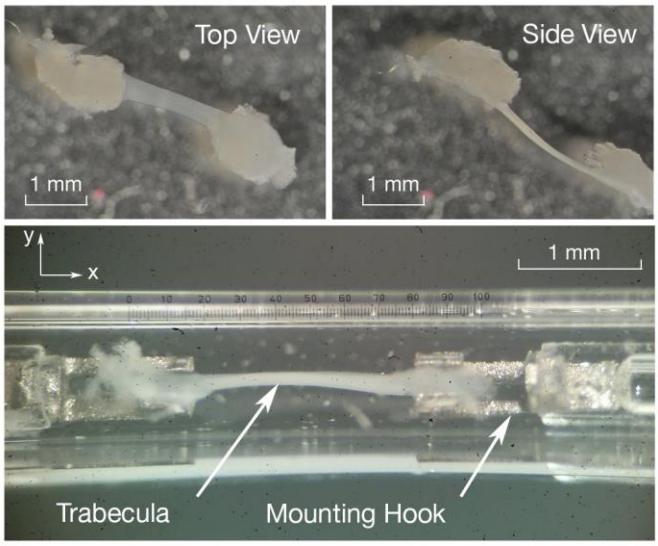

Figure 3. (Top) Two views of the trabecula sample imaged under a light microscope to show the ribbon shape. (Bottom) The same trabecula mounted in between two platinum hooks. The ends are trimmed to allow it to fit between the hooks.

E. Image Processing

The cross-sectional images (B-scans) were segmented using the LabView Vision Development Module (National Instruments) to estimate both the specimen's cross sectional area along its length and total volume between the mounting hooks. Each B-scan was first converted to a binary image with a threshold manually selected to maximize the inclusion of the sample of interest while minimizing the inclusion of background noise. Holes within objects were filled using the "fill holes" function in the package. Background particles were removed using the "remove small objects" function, which erodes the image six times with a square structuring element and removes the objects that are no longer present. In both cases, objects were defined as 8-connected neighbourhoods. Finally, open then close operations with a 5x5 hexagonal structuring element were used to smooth the edges of the trabecula. An illustration of this procedure is demonstrated in Figure 6.

The image processing steps resulted in segmented B-scans where the foreground pixels corresponded to the specimen. These pixels were counted to find the area of the trabecula cross-section, taking into account the calibrated pixel dimension and refractive index of the sample. Knowing the thickness of each slice, the slice volumes were summed to give the total volume of trabecula between the hooks.

IV. Results

A. Images

A single B-scan acquired between the mounting hooks is shown in Figure 4. The trabecula can clearly be resolved through the glass capillary using OCT, showing in this case a bent, elliptical cross section. The glass surfaces of the capillary and foreign particles such as dust are also visible around the trabecula. These do not affect the ability to process the image, however, as they do not overlap with the area of interest.

The volumetric image rendered using raw voxel data reveals higher level geometric features of the specimen in test (Figure 5). This includes slack in the specimen, slipping of the trabecula, and misalignment of hooks. This is useful for comparing the state of the mounted preparation between experiments.

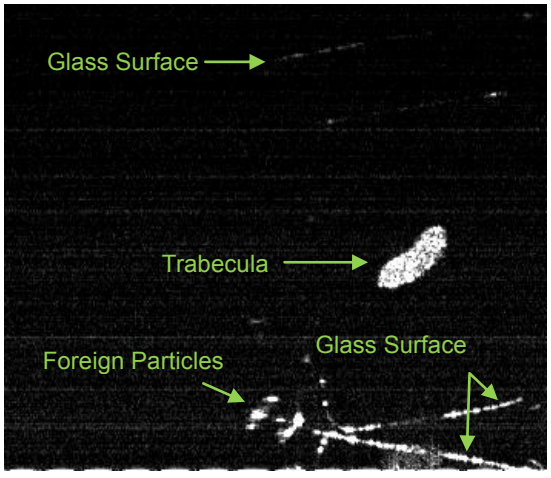

Figure 4. A B-scan of a trabecula inside the glass chamber, showing the glass capillary and other foreign particles.

B. Area and Volume Extraction

The result of the segmentation algorithm for a single B-scan shows that almost all of the artifacts can be removed using the procedure (Figure 6). This is consistent throughout the entire length of the trabecula between the hooks. The cross-sectional area and the total volume estimated using the described segmentation method are also shown in the figure. The values agree with estimates obtained from the microscope images shown in Figure 3, using the assumption of a uniform, elliptical cross section.

V. Discussion

The OCT images demonstrate that some trabeculae can be significantly non-cylindrical. It is important to capture this geometric information in order to better estimate the stresses and strains that develop across each sample. The OCT allows cross sectional images to be collected along the length of the trabecula, something a 2D microscope alone cannot do. We can later combine this geometric information with a sarcomere imaging system currently being developed to compare changes in sarcomere length distribution to the changes in bulk geometry of the specimen [12].

The focal plane of the imaging objective was aligned to have zero path difference with the reference arm, where the signal to noise ratio is the highest. In the B-scans presented, the surface of the trabecula is located 0.5 mm from the focal plane. For larger samples, it will be better to position the trabecula closer to the focal plane as signal strength fades with increasing depth (Figure 7). However, this will cause the mirror image of the glass capillary to overlap the image of the trabecula. This problem is inherent to Fourier domain OCT without phase correction. Further work will be done to

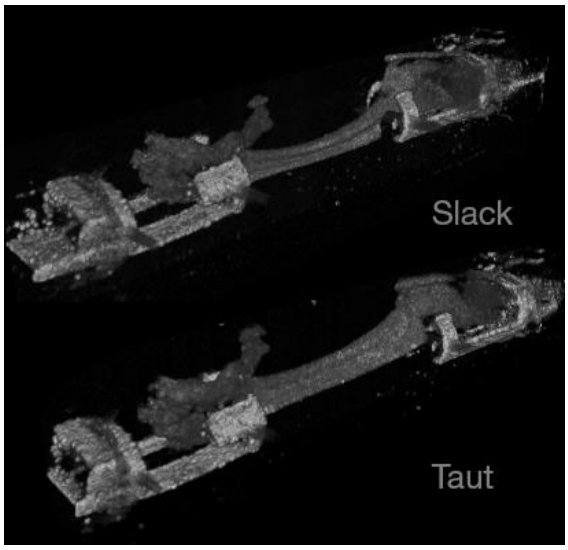

Figure 5. The rendered voxel data reveals higher level visual features of the mounted specimen. The image shows one instance where the trabecula is slack and one where it is taut. Slippage from hooks is visible in the taut case.

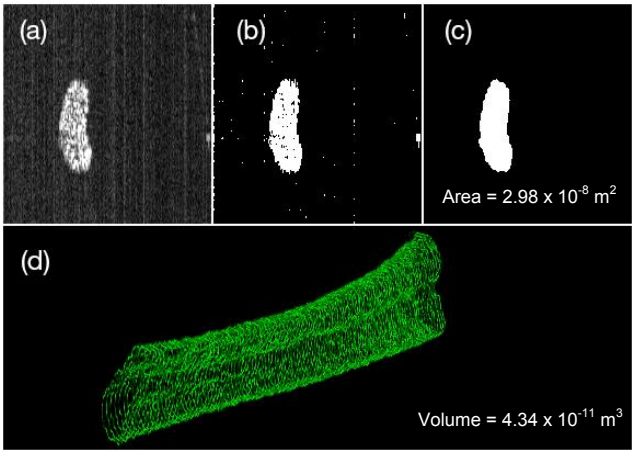

Figure 6. Image processing steps for calculating a volume from the trabecula B-Scans. (a) The region of interest is extracted. (b) The grayscale image is thresholded into a binary image. (c) Morphological operators are used to fill holes and remove small particles and the area is found by counting the foreground pixels. (d) The process is repeated down the length of the trabecula and the volume is calculated for the displayed section.

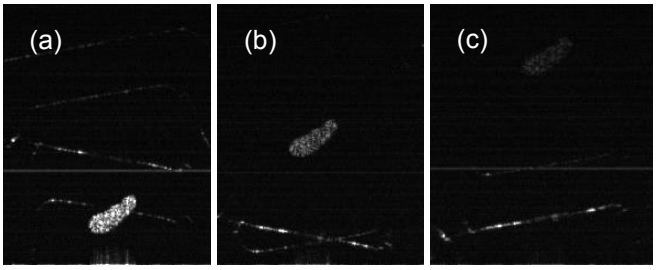

Figure 7. The trabecula at (a) 275 µm, (b) 760 µm, and (c) 1218 µm away from the focal plane (bottom of the image). This illustrates the reflections from the glass wall overlapping the trabecula when it is near the focal plane and the drop in the signal to noise ratio as the trabecula is moved further away.

reduce the magnitude of the signal reflected from the capillary, which will allow for imaging of the sample closer to the zero path difference

The image processing techniques described here use straightforward morphological operations on binary images which can be implemented to run very efficiently, enabling real time processing of area and volume during experiments. Future work will explore more sophisticated image segmentation algorithms, such as fitting an active contour model, which could improve estimates of the specimen boundaries. Furthermore, techniques for generating a mesh from segmented voxel data or surface point cloud will be implemented so that further finite element analysis can be performed on OCT data.

ACKNOWLEDGMENT

The authors thank Dr. Marie-Louise Ward and the Muscle Cell Function Research Group at the School of Medical Sciences for their assistance with obtaining and fixing the muscle preparations.

REFERENCES

[1] J.-C. Han, A. J. Taberner, R. S. Kirton, P. M. Nielsen, N. P. Smith, and D. S. Loiselle, "A unique micromechanocalorimeter for simultaneous measurement of heat rate and force production of cardiac trabeculae carneae.," *J. Appl. Physiol.*, vol. 107, no. 3, pp. 946–51, Sep. 2009.

[2] A. J. Taberner, "Cardiac Myometry: Multiple measurements of heart-muscle function," in *Medical Sciences Congress*, 2013.

[3] S. Goo, P. Joshi, G. Sands, D. Gerneke, A. Taberner, Q. Dollie, I. LeGrice, and D. Loiselle, "Trabeculae carneae as models of the ventricular walls: implications for the delivery of oxygen.," *J. Gen. Physiol.*, vol. 134, no. 4, pp. 339–50, Oct. 2009.

[4] J. G. Fujimoto, "Optical coherence tomography for ultrahigh resolution in vivo imaging.," *Nat. Biotechnol.*, vol. 21, no. 11, pp. 1361–7, Nov. 2003.

[5] M. Wojtkowski, V. Srinivasan, and T. Ko, "Ultrahigh-resolution, high-speed, Fourier domain optical coherence tomography and methods for dispersion compensation," *Opt. Express*, vol. 12, no. 11, pp. 707–709, 2004.

[6] Z. Yaqoob, J. Wu, and C. Yang, "Spectral domain optical coherence tomography: a better OCT imaging strategy," *Biotechniques*, vol. 39, no. 6 Suppl, pp. S6–13, Dec. 2005.

[7] N. Lippok, S. Coen, P. Nielsen, and F. Vanholsbeeck, "Dispersion compensation in Fourier domain optical coherence tomography using the fractional Fourier transform," *Opt. Express*, vol. 20, no. 21, pp. 1704–1706, 2012.

[8] A. Fercher and W. Drexler, "Optical coherence tomography-principles and applications," *Reports Prog. Phys.*, vol. 66, no. 2, pp. 239–303, 2003.

[9] A. Taberner, "An innovative work-loop calorimeter for in vitro measurement of the mechanics and energetics of working cardiac trabeculae," *J. Appl. Physiol.*, vol. 111, no. 6, pp. 1798–1803, 2011.

[10] A. N. Bashkatov, E. A. Genina, and V. V. Tuchin, "Optical Properties of Skin, Subcutaneous, and Muscle Tissues: a Review," *J. Innov. Opt. Health Sci.*, vol. 04, no. 01, pp. 9–38, Jan. 2011.

[11] X. Shen, M. B. Cannell, and M.-L. Ward, "Effect of SR load and pH regulatory mechanisms on stretch-dependent Ca(2+) entry during the slow force response.," *J. Mol. Cell. Cardiol.*, vol. 63, pp. 37–46, Oct. 2013.

[12] A. J. Anderson, P. M. F. Nielsen, and A. J. Taberner, "An investigation into the viability of image processing for the measurement of sarcomere length in isolated cardiac trabeculae.," *Conf. Proc. IEEE Eng. Med. Biol. Soc.*, vol. 2012, pp. 1566–9, Jan. 2012.